Structural optimization by the level-set method

Grégoire Allaire, François Jouve, Anca-Maria Toader

Abstract. In the context of structural optimization we describe a new numerical method based on a combination of the classical shape derivative and of the level-set method for front propagation. We implemented this method in two and three space dimensions for models of linear or non-linear elasticity, with various objective functions and contraints on the volume or on the perimeter. The shape derivative is computed by an adjoint method. The cost of our numerical algorithm is moderate since the shape is captured on a fixed Eulerian mesh. Although this method is not specifically designed for topology optimization, it can easily handle topology changes.

1. Introduction

Shape optimization of elastic structures is a very important and popular field. The classical method of shape sensitivity (or boundary variation) has been much studied (see e.g. [13], [16], [20], [21]). It is a very general method which can handle any type of objective functions and structural models, but it has two main drawbacks: its computational cost (because of remeshing) and its tendency to fall into local minima far away from global ones. The homogenization method (see e.g. [1], [2], [5], [7], [8], [12]) is an adequate remedy to these drawbacks but it is mainly restricted to linear elasticity and particular objective functions (compliance, eigenfrequency, or compliant mechanism). Recently yet another method appeared in [14], [18], [4] based on the level-set method which has been devised by Osher and Sethian [15], [17] for numerically tracking fronts and free boundaries. The level-set method is versatile and computationaly very efficient: it is by now a classical tool in many fields such as motion by mean curvature, fluid mechanics, image processing, etc.

The work [14] studied a two-phase optimization of a membrane (modelled by a linear scalar partial differential equation), i.e. the free boundary was the interface between two constituants occupying a given domain. It combined the level-set method with the shape sensitivity analysis framework. On the other hand, the work [18] focused on structural optimization within the context of two-dimensional linear elasticity. The shape of the structure was the free boundary which was captured on a fixed mesh using the immersed interface method. However, [18] did not rely on shape sensitivity analysis: rather the structural rigidity was improved by using an ad hoc criteria based on the Von Mises equivalent stress.

In [4] we generalized these two previous works in many aspects. Here we give a brief review of our approach based on a systematic implementation of the level-set method where the front velocity is derived from a shape sensitivity analysis. We focus on shape optimization rather than two-phase optimization, and we replace the immersed interface method by the simpler "ersatz material" approach which amounts to fill the holes by a weak phase. This is a well-known approach in topology optimization which can be rigorously justified in some cases [1]. We compute a shape derivative by using an adjoint problem. Then, the shape derivative is used as the normal velocity of the free boundary which is moved during the optimization process. Front propagation is performed by solving a Hamilton-Jacobi equation for a level-set function.

Acknowledgements: This work has been supported by the grant CNRS/ICCTI n^o 2002-12163 of the Centre National de la Recherche Scientifique (France) and the Instituto de Cooperação Científica e Tecnologica Internacional (Portugal).

2. Setting of the problem

We start by describing a model problem in linearized elasticity. There is no conceptual difficulty in choosing another model, and in particular a nonlinear elasticity problem. Let $\Omega \subset \mathbb{R}^d$ ($d = 2$ or 3) be a bounded open set occupied by a linear isotropic elastic material with Hooke's law A. Recall that, for any symmetric matrix ξ, A is defined by

$$A\xi = 2\mu\xi + \lambda\big(\mathrm{Tr}\xi\big)\,\mathrm{Id},$$

where μ and λ are the Lamé moduli of the material. The boundary of Ω is made of two disjoint parts

$$\partial\Omega = \Gamma_N \cup \Gamma_D,$$

with Dirichlet boundary conditions on Γ_D, and Neumann boundary conditions on Γ_N. The two boundary parts Γ_D and Γ_N are allowed to vary in the optimization process, although it is possible to fix some portion of it (see the numerical examples below).

We denote by f the vector-valued function of the volume forces and by g that of the surface loads. The displacement field u in Ω is the solution of the linearized elasticity system

$$\begin{cases} -\mathrm{div}\,(A\,e(u)) = f & \text{in } \Omega \\ u = 0 & \text{on } \Gamma_D \\ \big(A\,e(u)\big)n = g & \text{on } \Gamma_N. \end{cases} \tag{1}$$

Since Ω is varying during the optimization process, f and g must be known for all possible configuration of Ω. We therefore introduce a working domain D (a bounded open set of $\mathbb{R}^d$) which contains all admissible shapes Ω.

To give a precise mathematical meaning to (1), we choose $f \in L^2(D)^d$ and $g \in H^1(D)^d$ and we assume that $\Gamma_D \neq \emptyset$ (otherwise we should impose an equilibrium condition on f and g). In such case it is well known that (1) admits a unique solution in $H^1(\Omega)^d$.

The objective function is denoted by $J(\Omega)$. In this paper, we shall mostly focus on two possible choices of J (these are merely examples, and much more freedom is allowed). A first classical choice is the compliance (the work done by the load)

$$J_1(\Omega) = \int_\Omega f \cdot u \, dx + \int_{\Gamma_N} g \cdot u \, ds = \int_\Omega A\, e(u) \cdot e(u)\, dx, \tag{2}$$

which is very comon in rigidity maximization. A second choice is a least square error compared to a target displacement

$$J_2(\Omega) = \left(\int_\Omega k(x) |u - u_0|^\alpha dx \right)^{1/\alpha}, \tag{3}$$

which is a useful criterion for the design of compliant mechanisms [3], [19]. We assume $\alpha \geq 2$, $u_0 \in L^\alpha(D)$ and $k \in L^\infty(D)$, a non-negative given weighting factor. In both formulas (2) and (3), $u = u(\Omega)$ is the solution of (1). We define a set of admissible shapes that must be open sets contained in the working domain D and of fixed volume V

$$\mathcal{U}_{ad} = \left\{ \Omega \subset D \text{ such that } |\Omega| = V \right\}. \tag{4}$$

Our model problem of shape optimization is

$$\inf_{\Omega \in \mathcal{U}_{ad}} J(\Omega). \tag{5}$$

It is well known that the minimization problem (5) is usually not well posed on the set of admissible shapes defined by (4) (i.e. it has no solution). In order to obtain existence of optimal shapes some smoothness or geometrical or topological constraints are required. For example, a variant of (5) with a perimeter constraint turns out to be a well-posed problem (see [6]). More precisely, if $\ell > 0$ is a positive Lagrange multiplier, the the minimization problem

$$\inf_{\Omega \in \mathcal{U}_{ad}} \left(J(\Omega) + \int_{\partial\Omega} ds \right) \tag{6}$$

admits at least one optimal solution. There are other regularized variants of (5) which are well-posed and we refer to [9], [11] for such existence theories. Note that, even if existence is not an issue of the present paper, we shall work with a smoother subset of (4) in order to define properly a notion of shape derivative.

3. Shape derivative

In order to apply a gradient method to the minimization of (5) we recall a classical notion of shape derivative. This notion goes back, at least, to Hadamard, and many have contributed to its development (see e.g. the reference books [16], [21]). Here, we follow the approach of Murat and Simon [13], [20]. Starting from a smooth reference open set Ω, we consider domains of the type

$$\Omega_\theta = \big(\mathrm{Id} + \theta\big)(\Omega),$$

with $\theta \in W^{1,\infty}(\mathbb{R}^d, \mathbb{R}^d)$. It is well known that, for sufficiently small θ, $(\mathrm{Id} + \tau)$ is a diffeomorphism in $\mathbb{R}^d$.

Definition 3.1. *The shape derivative of $J(\Omega)$ at Ω is defined as the Fréchet derivative in $W^{1,\infty}(\mathbb{R}^d, \mathbb{R}^d)$ at 0 of the application $\theta \to J\big((\mathrm{Id} + \theta)(\Omega)\big)$, i.e.*

$$J\big((\mathrm{Id} + \theta)(\Omega)\big) = J(\Omega) + J'(\Omega)(\theta) + o(\theta) \quad \text{with} \quad \lim_{\theta \to 0} \frac{\|o(\theta)\|}{\|\theta\|} = 0\,,$$

where $J'(\Omega)$ is a continuous linear form on $W^{1,\infty}(\mathbb{R}^d, \mathbb{R}^d)$.

A classical result states that the directional derivative $J'(\Omega)(\theta)$ depends only on the normal trace $\theta \cdot n$ on the boundary $\partial\Omega$.

Lemma 3.2. *Let Ω be a smooth bounded open set and $J(\Omega)$ a differentiable function at Ω. Its derivative satisfies*

$$J'(\Omega)(\theta_1) = J'(\Omega)(\theta_2)$$

if $\theta_1, \theta_2 \in W^{1,\infty}(\mathbb{R}^d; \mathbb{R}^d)$ are such that $\theta_2 - \theta_1 \in C^1(\mathbb{R}^d; \mathbb{R}^d)$ and

$$\theta_1 \cdot n = \theta_2 \cdot n \qquad \text{on } \partial\Omega.$$

We give two examples of shape derivative that will be useful in the sequel

Lemma 3.3. *Let Ω be a smooth bounded open set and $f(x) \in W^{1,1}(\mathbb{R}^d)$. Define*

$$J(\Omega) = \int_\Omega f(x)\, dx.$$

Then J is differentiable at Ω and

$$J'(\Omega)(\theta) = \int_\Omega \mathrm{div}\big(\theta(x)\, f(x)\big)\, dx = \int_{\partial\Omega} \theta(x) \cdot n(x)\, f(x)\, ds$$

for any $\theta \in W^{1,\infty}(\mathbb{R}^d; \mathbb{R}^d)$.

Lemma 3.4. *Let Ω be a smooth bounded open set and $f(x) \in W^{2,1}(\mathbb{R}^d)$. Define*

$$J(\Omega) = \int_{\partial\Omega} f(x)\, ds.$$

Then J is differentiable at Ω and

$$J'(\Omega)(\theta) = \int_{\partial\Omega} \theta \cdot n \left(\frac{\partial f}{\partial n} + Hf\right) ds,$$

for any $\theta \in W^{1,\infty}(\mathbb{R}^d; \mathbb{R}^d)$, where H is the mean curvature of $\partial\Omega$ defined by $H =$ div$n$.

Remark 3.5. *In particular Lemma 3.3 is useful in order to compute the shape derivative of a volume constraint* $V(\Omega) = C$. *Indeed, we have*

$$V(\Omega) = \int_\Omega dx \quad \textit{and} \quad V'(\Omega)(\theta) = \int_{\partial\Omega} \theta(x) \cdot n(x)\, ds.$$

Similarly, Lemma 3.4 is useful in order to compute the shape derivative of a perimeter constraint $P(\Omega) = C$. *Indeed, we have*

$$P(\Omega) = \int_{\partial\Omega} ds \quad \textit{and} \quad P'(\Omega)(\theta) = \int_{\partial\Omega} \theta(x) \cdot n(x) H\, ds.$$

Theorem 3.6. *Let* Ω *be a smooth bounded open set and* $\theta \in W^{1,\infty}(\mathbb{R}^d;\mathbb{R}^d)$. *The shape derivative of (2) is*

$$J_1'(\Omega)(\theta) = \int_{\partial\Omega} \left(2\left[\frac{\partial(g\cdot u)}{\partial n} + Hg\cdot u \right] - Ae(u)\cdot e(u) \right) \theta \cdot n\, ds. \tag{7}$$

The shape derivative of (3) is

$$J_2'(\Omega)(\theta) = \int_{\partial\Omega} \left(\frac{\partial(g\cdot p)}{\partial n} + Hg\cdot p - Ae(p)\cdot e(u) + \frac{C_0}{\alpha} k|u-u_0|^\alpha \right) \theta\cdot n\, ds, \tag{8}$$

where u *is the solution of (1), and* p *is the adjoint state, solution of*

$$\begin{cases} -\mathrm{div}\,(A\,e(p)) = C_0 k(x)|u-u_0|^{\alpha-2}(u-u_0) & \textit{in } \Omega \\ p = 0 & \textit{on } \Gamma_D \\ \big(Ae(p)\big)n = 0 & \textit{on } \Gamma_N, \end{cases} \tag{9}$$

where C_0 *is a constant given by*

$$C_0 = \left(\int_\Omega k(x)|u(x)|^\alpha dx \right)^{1/\alpha - 1}.$$

Remark 3.7. *Remark that there is no adjoint state involved in (7) (indeed the minimization of (2) is a self-adjoint problem).*

Proof. Although Theorem 3.6 is a classical result (see e.g. [13], [16], [20], [21]) we briefly sketch its proof for the sake of completeness. To simplify we give a short, albeit formal, proof due to Céa [10]. We consider a general objective function

$$J(\Omega) = \int_\Omega j(x,u)\, dx,$$

for which we introduce the Lagrangian defined for $(v,q) \in \big(H^1(\mathbb{R}^d;\mathbb{R}^d)\big)^2$ by

$$\begin{aligned} \mathcal{L}(\Omega, v, q) = & \int_\Omega j(x,v)\, dx + \int_\Omega Ae(v)\cdot e(q)\, dx - \int_\Omega q\cdot f\, dx \\ & - \int_{\Gamma_N} q\cdot g\, ds - \int_{\Gamma_D} \Big(q\cdot Ae(v)n + v\cdot Ae(q)n \Big) ds. \end{aligned} \tag{10}$$

In (10) q is a Lagrange multiplier for the state equation and its boundary conditions. It is worth noticing that v and q belong to a functional space that does not depend on Ω, so we can apply the usual differentation rule to the Lagrangian $\mathcal{L}$.

The stationarity of the Lagrangian is going to give the optimality conditions of the minimization problem. For a given Ω, we denote by (u,p) such a stationary point. The partial derivative of $\mathcal{L}$ with respect to q, in the direction $\phi \in H^1(\mathbb{R}^d;\mathbb{R}^d)$, after integration by parts leads to

$$\begin{aligned}\langle\frac{\partial\mathcal{L}}{\partial q}(\Omega,u,p),\phi\rangle = 0 = \quad & -\int_\Omega \phi\cdot\Big(\mathrm{div}(Ae(u))+f\Big)dx \\ & +\int_{\Gamma_N}\phi\cdot\big((Ae(u))n-g\big)\,ds \\ & -\int_{\Gamma_D} u\cdot Ae(\phi)n\,ds.\end{aligned} \tag{11}$$

Taking first ϕ with compact support in Ω gives the state equation. Then, varying the trace function ϕ on Γ_N gives the Neumann boundary condition for u, while varying the corresponding normal stress $\big(Ae(\phi)\big)n$ on Γ_D gives the Dirichlet boundary condition for u. On the other hand, in order to find the adjoint equation, we differentiate $\mathcal{L}$ with respect to v in the direction $\phi \in H^1(\mathbb{R}^d;\mathbb{R}^d)$. This yields

$$\begin{aligned}\langle\frac{\partial\mathcal{L}}{\partial v}(\Omega,u,p),\phi\rangle = 0 \quad &= \int_\Omega j'(u)\cdot\phi\,dx + \int_\Omega Ae(\phi)\cdot e(p)\,dx \\ & -\int_{\Gamma_D}\Big(p\cdot Ae(\phi)n+\phi\cdot Ae(p)n\Big)\,ds.\end{aligned}$$

Integrating by parts we obtain

$$\begin{aligned}\langle\frac{\partial\mathcal{L}}{\partial v}(\Omega,u,p,\mu),\phi\rangle = \quad & \int_\Omega \Big(j'(u)-\mathrm{div}(Ae(p))\Big)\cdot\phi\,dx + \int_{\Gamma_N}\phi\cdot\big(Ae(p)\big)n\,ds \\ & -\int_{\Gamma_D} p\cdot Ae(\phi)n\,ds.\end{aligned}$$

Taking first ϕ with compact support in Ω gives the adjoint state equation

$$-\mathrm{div}(Ae(p)) = -j'(u) \quad \text{in} \quad \Omega.$$

Then, varying the trace of ϕ on Γ_N yields the Neumann boundary condition

$$\big(Ae(p)\big)n = 0 \quad \text{on} \quad \Gamma_N.$$

Finally, varying the normal stress $\big(Ae(\phi)\big)n$ on Γ_D gives

$$p = 0 \quad \text{on} \quad \Gamma_D.$$

We have therefore find a well-posed boundary value problem for the adjoint state p.

The shape derivative of the objective function is obtained by differentiating

$$J(\Omega) = \mathcal{L}(\Omega,u(\Omega),p(\Omega)),$$

which, by the chain rule theorem, reduces to the partial derivative of $\mathcal{L}$ with respect to Ω in the direction θ

$$J'(\Omega)(\theta) = \frac{\partial\mathcal{L}}{\partial\Omega}(\Omega,u,p)(\theta).$$

Applying Lemma 3.3 and 3.4 we obtain

$$\begin{aligned}\frac{\partial \mathcal{L}}{\partial \Omega}(\Omega, u, p)(\theta) = & \int_{\partial\Omega} \theta \cdot n \Big(j(u) + Ae(u) \cdot e(p) - p \cdot f \Big) ds \\ & - \int_{\Gamma_N} \theta \cdot n \left(\frac{\partial (g \cdot p)}{\partial n} + H\, g \cdot p \right) ds \\ & - \int_{\Gamma_D} \theta \cdot n \left(\frac{\partial h}{\partial n} + Hh \right) ds,\end{aligned} \tag{12}$$

with $h = u \cdot Ae(p)n + p \cdot Ae(u)n$. Taking into account the boundary condition $u = p = 0$ on Γ_D which also implies

$$Ae(u) \cdot e(p) = \mu \frac{\partial u}{\partial n} \cdot \frac{\partial p}{\partial n} + (\mu + \lambda) \left(\frac{\partial u}{\partial n} \cdot n \right) \left(\frac{\partial p}{\partial n} \cdot n \right) \quad \text{on } \Gamma_D,$$

we deduce

$$\begin{aligned}\frac{\partial \mathcal{L}}{\partial \Omega}(\Omega, u, p)(\theta) = & \int_{\Gamma_N} \theta \cdot n \left(j(u) + Ae(u) \cdot e(p) - \frac{\partial (g \cdot p)}{\partial n} - H\, g \cdot p \right) ds \\ & + \int_{\Gamma_D} \theta \cdot n \Big(j(u) - Ae(u) \cdot e(p) \Big) ds.\end{aligned}$$

This proof is merely a formal computation (in particular it assumes that u and p are differentiable with respect to the shape Ω) but it can be rigorously justified (see the references quoted above). □

Remark 3.8. *We can generalize Theorem 3.6 to more general objective functions, including functions of the strain or stress. It is also possible to consider non homogeneous Dirichlet boundary conditions in the state equation, or even a non-linear model of elasticity.*

Remark 3.9. *It is possible to further restrict the class of domains by asking that some parts of the boundary Γ_{fixed} do not move: specifically, the map θ must belong to*

$$T_{ad} = \left\{ \theta \in W^{1,\infty}(\mathbb{R}^d, \mathbb{R}^d) \text{ such that } \theta = 0 \text{ on } \Gamma_{fixed} \right\}.$$

4. Front propagation by the level-set method

Let a bounded domain $D \subset \mathbb{R}^d$ be the working domain in which all admissible shapes Ω are included, i.e. $\Omega \subset D$. In numerical practice, the domain D will be uniformly meshed once and for all. Then, we shall capture the shape Ω on this fixed mesh. For this purpose, we parametrize the boundary of Ω by means of a level-set function, following the idea of Osher and Sethian [15]. We define this level-set function ψ in D such that

$$\begin{cases} \psi(x) = 0 & \Leftrightarrow x \in \partial\Omega \cap D \\ \psi(x) < 0 & \Leftrightarrow x \in \Omega \\ \psi(x) > 0 & \Leftrightarrow x \in (D \setminus \Omega) \end{cases}$$

The normal n to the shape Ω is recovered as $\nabla\psi/|\nabla\psi|$ and the curvature H is given by the divergence of n (these quantities are evaluated by finite differences since our mesh is uniformly rectangular). Remark that, although n and H are theoretically defined only on $\partial\Omega$, the level set method allows to define easily their extension in the whole domain D.

Following the optimization process, the shape is going to evolve according to a ficititious time which corresponds to descent stepping (we shall come back to issue in the next section). As is well-known, if the shape is evolving in time, then the evolution of the level-set function is governed by a simple Hamilton-Jacobi equation. To be precise, assume that the shape $\Omega(t)$ evolves in time $t \in \mathbb{R}^+$ with a normal velocity $V(t, x)$. Then

$$\psi\Big(t, x(t)\Big) = 0 \quad \text{for any } x(t) \in \partial\Omega(t).$$

Differentiating in t yields

$$\frac{\partial\psi}{\partial t} + \dot{x}(t) \cdot \nabla_x\psi = \frac{\partial\psi}{\partial t} + Vn \cdot \nabla_x\psi = 0.$$

Since $n = \nabla_x\psi/|\nabla_x\psi|$ we obtain

$$\frac{\partial\psi}{\partial t} + V|\nabla_x\psi| = 0.$$

This Hamilton Jacobi equation is posed in the whole box D, and not only on the boundary $\partial\Omega$, if the velocity V is known everywhere. Remark that the level-set method easily allows to compute the mean curvature $H = \mathrm{div}n$ (which plays an important role in a perimeter penalization).

It is solved by an explicit first order upwind scheme (see e.g. [17])

$$\frac{\psi_i^{n+1} - \psi_i^n}{\Delta t} + \min(V_i^n, 0)\, g^-(D_x^+\psi_i^n, D_x^-\psi_i^n) + \max(V_i^n, 0)\, g^+(D_x^+\psi_i^n, D_x^-\psi_i^n) = 0$$

with $D_x^+\psi_i^n = \frac{\psi_{i+1}^n - \psi_i^n}{\Delta x}$, $D_x^-\psi_i^n = \frac{\psi_i^n - \psi_{i-1}^n}{\Delta x}$, and

$$g^+(d^+, d^-) = \sqrt{\min(d^+, 0)^2 + \max(d^-, 0)^2},$$

$$g^-(d^+, d^-) = \sqrt{\max(d^+, 0)^2 + \min(d^-, 0)^2}.$$

In order to regularize the level set function (which may become too flat or too steep), we reinitialize it periodically by solving

$$\begin{cases} \frac{\partial\psi}{\partial t} + \mathrm{sign}(\psi)\Big(|\nabla_x\psi| - 1\Big) = 0 & \text{in } D \times \mathbb{R}^+, \\ \psi(t = 0, x) = \psi_0(x) & \text{in } D, \end{cases} \tag{13}$$

which admits as a stationary solution the signed distance to the initial interface $\{\psi_0(x) = 0\}$. In numerical practice, reinitialization is very important because the level set function often becomes too steep which implies a bad approximation of the normal n or of the curvature H.

5. Optimization algorithm

For the minimization problem

$$\inf_{\Omega \in \mathcal{U}_{ad}} \left\{ J(\Omega) = \int_\Omega j(x,u)\, dx \right\}$$

we computed a shape derivative

$$J'(\Omega)(\theta) = \int_{\partial\Omega} v\, \theta \cdot n\, ds,$$

where the function v is given by a result like Theorem 3.6. Ignoring smoothness issues, a descent direction is found by taking

$$\theta = -v\, n.$$

The normal component $\theta \cdot n = -v$ is therefore our choice of advection velocity in the Hamilton-Jacobi equation

$$\frac{\partial \psi}{\partial t} - v|\nabla\psi| = 0. \tag{14}$$

Transporting ψ by (14) is equivalent to move the boundary of Ω (the zero level set of ψ) along the descent gradient direction $-J'(\Omega)$. Finally, our algorithm is an iterative method, structured as follows:

1. Initialization of the level-set function ψ_0 corresponding to an initial guess Ω_0.
2. Iteration until convergence, for $k \geq 0$:
   (a) Computation of the state u_k and adjoint state p_k through two problems of linear elasticity.
   (b) Deformation of the shape through the transport of the level set function: $\psi_{k+1}(x) = \psi(\Delta t_k, x)$ where $\psi(t,x)$ is the solution of (14) with velocity $v_k = v(u_k, p_k)$ and initial condition $\psi(0,x) = \psi_k(x)$. The time step Δt_k is chosen such that $J(\Omega_{k+1}) \leq J(\Omega_k)$.
3. From time to time, for stability reasons, we also reinitialize the level set function ψ by solving (13).

In order to avoid an explicit meshing of the shapes Ω_k, we compute the state u_k and adjoint state p_k in the whole working domain D. For this, we fill the void part $D \setminus \Omega_k$ with a very weak material with Hooke's law $B = 10^{-3}A$ and we perform the elasticity analysis on a fixed rectangular mesh in D (using $Q1$ finite elements). Then, the Hooke's law in D is

$$A_k(x) = \begin{cases} A & \text{where } \psi_k(x) < 0 \\ 10^{-3}A & \text{where } \psi_k(x) > 0, \end{cases}$$

completed by a simple linear interpolation (proportional to the volume) of these values in the mesh cells where ψ_k changes sign.

Since n and H, as well as the state u and the adjoint state p, are computed everywhere in D, the shape derivative (see formulas (7) and (8)) delivers a normal velocity $-v$ which is defined throughout the domain D and not only on the free boundary $\partial\Omega$. Therefore, we never have to know where precisely is the boundary $\partial\Omega$ and we apply the same numerical scheme everywhere in the working domain D.

Since the Hamilton-Jacobi equation (14) is solved by an explicit scheme, the time step Δt_k must satisfy a CFL condition. Remark that one explicit time step for (14) is much cheaper, in terms of CPU time and memory requirement, than the solution of the state equation (1) or adjoint state equation (9). On the other hand, the usual time step Δt_k for (14) is often much smaller that the optimal descent step for the minimization of the objective function $J(\Omega)$. Therefore, for each iteration k in the above algorithm (corresponding to a single evaluation of u_k and p_k), we solve several time steps of the Hamilton-Jacobi equation (14). The number of such time steps per iteration k is monitored by the decrease of $J(\Omega_k)$.

Our algorithm never creates new holes or boundaries if the time step Δt_k does indeed satisfy a CFL condition because of the mxximum principle for (14) (there is no nucleation mechanism for new holes). However the level set method is well known to handle easily topology changes, i.e. merging or cancellation of holes. Therefore, our algorithm is able to perform topology optimization if the number of holes of the initial design is sufficiently large (see Figure 1). The algorithm converges smoothly to a (local) minimum which strongly depends, of course, on the initial topology (see the differences in Figures 2 and 3). For a “good” initialization, the numerical results are very similar to those obtained by the homogenization method but the convergence is usually slower (although we did not yet try to speed it by a quasi-Newton algorithm).

6. Numerical examples

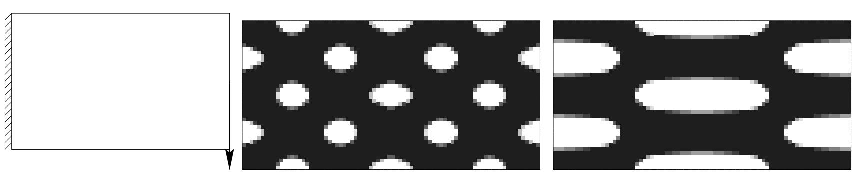

FIGURE 1. Boundary conditions and two initializations of a 2-d cantilever

We first consider a compliance problem and neglect body forces, i.e. $f \equiv 0$ in (1). The objective function is a combination of the compliance and of the weight of the structure

$$J(\Omega) = \int_{\Gamma_N} g \cdot u \, ds + \ell \int_{\Omega} dx, \tag{15}$$

where $\ell > 0$ is a Lagrange multiplier. We further impose that the Dirichlet boundary Γ_D, as well as that part of the Neumann boundary Γ_N where the loads are applied are kept fixed during the homogenization process. Thus, only the traction-free Neumann boundary is allowed to move. The boundary conditions and two initial configurations for a plane cantilever are displayed on Figure 1. The results are shown on Figures 2 and 3 for two different iteration number, showing the strong influence of the initialization. The convergence is smooth and fast (see Figure 4) and 20 explicit time steps of the Hamilton-Jacobi equation were performed at each elasticity iteration.

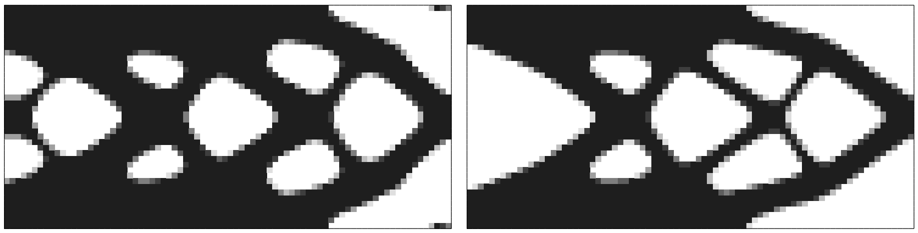

FIGURE 2. Iterations 10 and 50 of the two-dimensional cantilever initialized as in Figure 1 (middle)

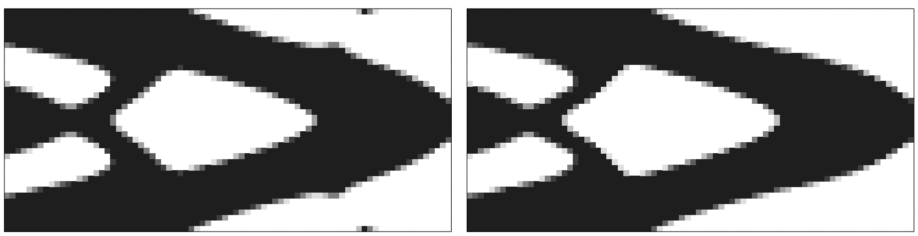

FIGURE 3. Iterations 10 and 50 of the two-dimensional cantilever initialized as in Figure 1 (right)

The advantage of the level-set method is that it can be easily extended to three space dimensions. A three-dimensional optimal electrical mast is given on Figure 5 (see [2] for a precise definition of this test case).

Next, Figure 6 shows a numerical result for the least square objective function (3) where $k(x)$ and $u_0(x)$ have been chosen such that the jaws of the mechanisme close. This is a classical gripping mechanism test case which is described, e.g., in [1], [19].

We come back to the compliance objective function (2) with design dependent loads and take g as a uniform pressure load on the free-boundary Γ_N. Imposing 5 Dirichlet points yields a nice sea star as can be seen of Figure 7.

Our shape optimization method can easily be extended to models of non-linear elasticity or to multiple loads problem. This, as well as the study of the effect of first-order or second-order discretization and of re-initialization in the

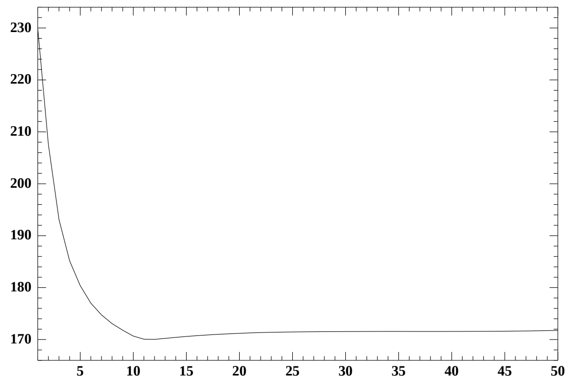

FIGURE 4. Convergence of the objective function for the two-dimensional cantilever of Figure 3

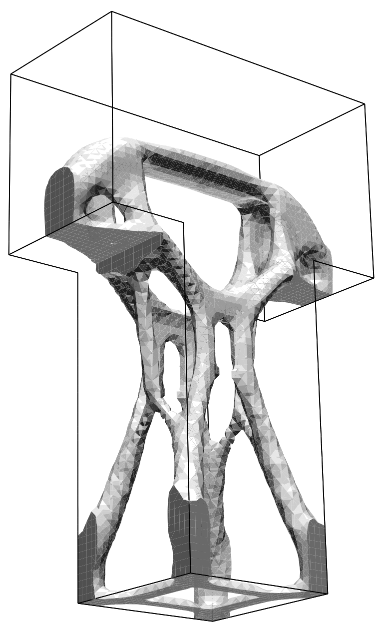

FIGURE 5. Three-dimensional electrical mast.

numerical convergence towards an optimal shape, are the subject of a forthcoming paper.

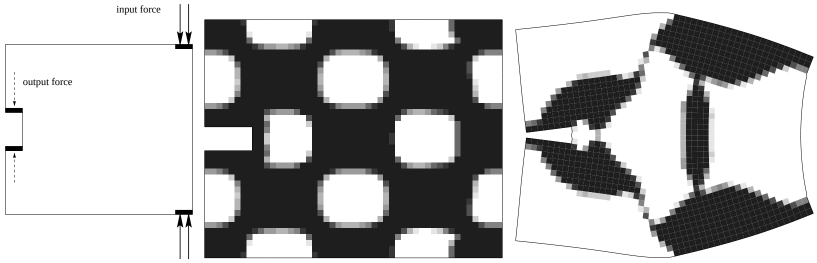

FIGURE 6. Boundary conditions, initialization, and deformed optimal shape of a plane gripping mechanism.

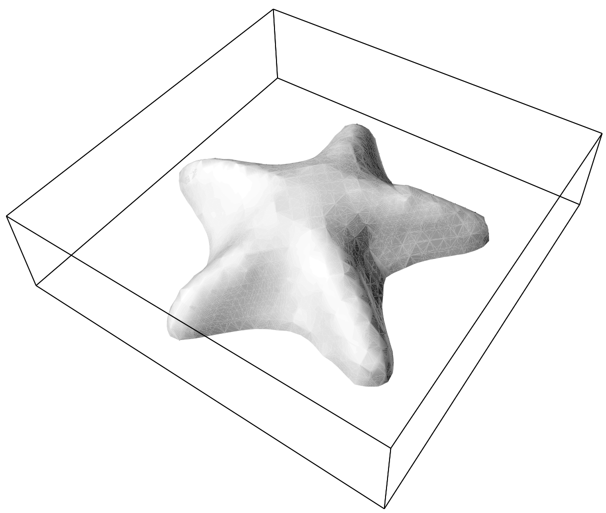

FIGURE 7. Optimal shape under a uniform pressure load with five anchor points.

References

[1] G. Allaire, *Shape optimization by the homogenization method*, Springer Verlag, New York, (2001).

[2] G. Allaire, E. Bonnetier, G. Francfort, F. Jouve, *Shape optimization by the homogenization method.* Nümerische Mathematik, **76**, 27–68, (1997).

[3] G. Allaire, F. Jouve, *Optimal design of micro-mechanisms by the homogenization method*, European Journal of Finite Elements, **11**, 405–416 (2002).

[4] G. Allaire, F. Jouve, A.-M. Toader, *A level-set method for shape optimization,* C. R. Acad. Sci. Paris, Série I, **334**, 1125–1130 (2002).

[5] G. Allaire, R.V. Kohn, *Optimal design for minimum weight and compliance in plane stress using extremal microstructures,* Europ. J. Mech. A/Solids, **12**, 6, 839–878, (1993).

[6] L. Ambrosio , G. Buttazzo, *An optimal design problem with perimeter penalization,* Calc. Var. **1**, 55–69 (1993).

[7] M. Bendsoe, *Methods for optimization of structural topology, shape and material,* Springer Verlag, New York, (1995).

[8] M. Bendsoe, N. Kikuchi, *Generating Optimal Topologies in Structural Design Using a Homogenization Method,* Comp. Meth. Appl. Mech. Eng., **71**, 197–224, (1988).

[9] A. Chambolle, *A density result in two-dimensional linearized elasticity and applications,* Preprint CEREMADE 121, Université Paris-Dauphine, (2001).

[10] J. Céa, *Conception optimale ou identification de formes, calcul rapide de la dérivée directionnelle de la fonction coût,* Math. Model. Num. Anal., **20**, 3, 371–402 (1986).

[11] D. Chenais, *On the existence of a solution in a domain identification problem,* J. Math. Anal. Appl. **52**, 189–289 (1975).

[12] A. Cherkaev A., *Variational Methods for Structural Optimization,* Springer Verlag, New York (2000).

[13] F. Murat, S. Simon, *Etudes de problèmes d'optimal design,* Lecture Notes in Computer Science **41**, 54–62, Springer Verlag, Berlin, (1976).

[14] S. Osher, F. Santosa, *Level set methods for optimization problems involving geometry and constraints: frequencies of a two-density inhomogeneous drum,* J. Comp. Phys., **171**, 272–288, (2001).

[15] S. Osher, J.A. Sethian, *Front propagating with curvature dependent speed: algorithms based on hamilton-jacobi formulations,* J. Comp. Phys., **78**, 12–49, (1988).

[16] O. Pironneau, *Optimal shape design for elliptic systems,* Springer-Verlag, New York, (1984).

[17] J.A. Sethian, *Level Set Methods and fast marching methods: evolving interfaces in computational geometry, fluid mechanics, computer vision and materials science,* Cambridge University Press, (1999).

[18] J.A. Sethian, A. Wiegmann, *Structural boundary design via level set and immersed interface methods,* J. Comp. Phys., **163**, 489–528, (2000).

[19] O. Sigmund, *On the design of compliant mechanisms using topology optimization,* Mech. Struct. Mach., **25**, 493–524 (1997).

[20] J. Simon, *Differentiation with respect to the domain in boundary value problems,* Num. Funct. Anal. Optimz., **2**, 649–687, (1980).

[21] J. Sokolowski, J.P. Zolesio, *Introduction to shape optimization: shape sensitity analysis*, Springer Series in Computational Mathematics, Vol. 10, Springer, Berlin, (1992).

Centre de Mathématiques Appliquées,
Ecole Polytechnique,
91128 Palaiseau, France

CMAF, Faculdade de Ciências da Universidade de Lisboa,
Av. Prof. Gama Pinto 2, 1699 Lisboa, Portugal
E-mail address: gregoire.allaire@polytechnique.fr, francois.jouve@polytechnique.fr, amtan@lmc.fc.ul.pt